

LETTER • **OPEN ACCESS**

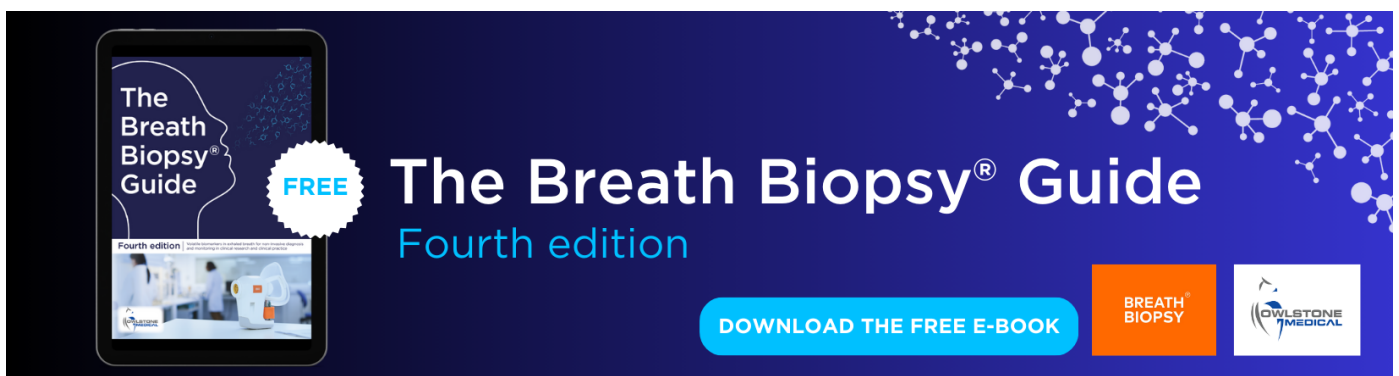
Flash drought development and cascading impacts associated with the 2010 Russian heatwave

To cite this article: Jordan I Christian *et al* 2020 *Environ. Res. Lett.* **15** 094078

View the [article online](#) for updates and enhancements.

You may also like

- [Regional characteristics of flash droughts across the United States](#)
Jordan I Christian, Jeffrey B Basara, Jason A Otkin *et al.*
- [Increasing risk of simultaneous occurrence of flash drought in major global croplands](#)
Shanti Shwarup Mahto and Vimal Mishra
- [The evolution, propagation, and spread of flash drought in the Central United States during 2012](#)
Jeffrey B Basara, Jordan I Christian, Ryann A Wakefield *et al.*



The Breath Biopsy® Guide
Fourth edition

FREE

DOWNLOAD THE FREE E-BOOK

BREATH BIOPSY

OWLSTONE MEDICAL

Environmental Research Letters



LETTER

OPEN ACCESS

RECEIVED
10 April 2020

REVISED
10 June 2020

ACCEPTED FOR PUBLICATION
24 June 2020

PUBLISHED
28 August 2020

Original content from this work may be used under the terms of the [Creative Commons Attribution 4.0 licence](#). Any further distribution of this work must maintain attribution to the author(s) and the title of the work, journal citation and DOI.



Flash drought development and cascading impacts associated with the 2010 Russian heatwave

Jordan I Christian¹ , Jeffrey B Basara^{1,2} , Eric D Hunt³ , Jason A Otkin⁴ and Xiangming Xiao⁵

¹ School of Meteorology, University of Oklahoma, Norman, OK 73072, United States of America

² School of Civil Engineering and Environmental Science, University of Oklahoma, Norman, OK 73019, United States of America

³ Atmospheric and Environmental Research, Inc., Lexington, MA 02421, United States of America

⁴ Cooperative Institute for Meteorological Satellite Studies, Space Science and Engineering Center, University of Wisconsin-Madison, Madison, WI 53706, United States of America

⁵ Department of Microbiology and Plant Biology, Center of Spatial Analysis, University of Oklahoma, Norman, OK 73019, United States of America

E-mail: jchristian@ou.edu

Keywords: flash drought, heatwave, evapotranspiration, enhanced vegetation index

Supplementary material for this article is available [online](#)

Abstract

The 2010 western Russian heatwave was characterized by historically high surface temperatures that led to devastating impacts on the environment, economy, and society. Recent studies have attributed a quasi-stationary upper level ridge, sensible heat advection, and land-atmosphere temperature coupling as the primary components for the development of the heatwave event. The results in this study reveal that rapid drought intensification occurred prior to the extreme atmospheric conditions associated with the heatwave. The flash drought event developed from a lack of rainfall coupled with enhanced evaporative demand and resulted in rapid desiccation of the land surface. The region that underwent rapid drought intensification acted to prime the land-atmosphere interactions necessary to supplement the excessive surface temperatures experienced during the heatwave event. This area also provided a source region for the advection of warm, dry air to promote heatwave development downwind of the flash drought location. As such, the hydrometeorological extremes associated with the precursor flash drought and heatwave resulted in cascading impacts that severely affected ecosystems, agriculture, and human health. Given the findings from this research, we conclude that flash drought impacts should be expanded beyond vegetative and agricultural applications and should be viewed as a possible precursor and direct forcing for heatwave events and associated impacts.

1. Introduction

The 2010 heatwave across western Russia was an extreme event that led to profound environmental, economic, and societal impacts. In the agricultural sector, grain yields were severely impacted, as the 'wheat belt' extending across southwestern Russia (the Central and Volga federal districts) experienced grain harvests that were less than half of what they were the previous year (Wegren 2011). As a result, the Russian government imposed an export ban on wheat in August 2010 that significantly increased its price in the global market (Welton 2011). Due to environmental conditions that included anomalously high surface temperatures and vapor pressure

deficits, large wildfires were also prevalent. Thousands of people were displaced due to catastrophic loss of property (Bondur 2011) and severe air pollution from the fires significantly increased mortality during the late summer when the spatial extent of the wildfires was at its peak (Shaposhnikov *et al* 2014). In all, the resulting impacts associated with the heatwave event led to a total of approximately 11 000 excess deaths (i.e. a near 20% increase in deaths for the given time period; Shaposhnikov *et al* 2014).

Placed in historical context, the summer of 2010 was likely one of the warmest for Europe and western Russia in the last half millennium (Barriopedro *et al* 2011). Record-high surface temperatures exceeding 32°C were reached for Moscow and the surrounding

region by mid- to late July and persisted until the second week of August (Barriopedro *et al* 2011, Grumm 2011). Three primary meteorological components have been connected to the development and propagation of the heatwave event: (1) a quasi-stationary upper-level ridge centered over western Russia during July and August (Barriopedro *et al* 2011, Grumm 2011), (2) sensible heat advection (Schumacher *et al* 2019), and (3) land-atmosphere temperature coupling via heat storage in nocturnal residual layers (Miralles *et al* 2014). The subsidence from the associated upper-level synoptic environment inhibited precipitation throughout most of the summer (figure 1) while persistent desiccation of the land surface occurred due to high evaporative demand. Sensible heat associated with desiccated soils southeast of the primary heatwave region were advected northwestward and augmented the local sensible heat flux (Schumacher *et al* 2019). In addition, progressive accumulation of heat in the boundary layer amplified the above-average surface temperatures (Miralles *et al* 2014) already set in place by the overlying synoptic environment and land surface conditions.

This study expands upon the knowledge of the 2010 heatwave by linking the desiccated land surface and resulting sensible heat advection associated with the heatwave to a critical precursor subseasonal phenomenon: flash drought. Flash droughts are uniquely defined by their rapid rate of intensification toward drought conditions (Otkin *et al* 2018). When a combination of environmental anomalies drive persistent, enhanced evaporative demand for several weeks, rapid depletion of available soil moisture will occur. As evapotranspiration (ET) from the land surface diminishes, the partitioning of surface energy fluxes contributes to a decreased evaporative fraction. Consequently, low values of evaporative fraction correspond with a decreased efficiency to moderate land surface temperatures and the resulting increase in evaporative demand will exacerbate the moisture stress on the environment. This process associated with rapid drought development directly impacts ecosystem health and agriculture productivity, such as was observed during the expansive flash drought across the Great Plains in 2012 that led to \$30 billion in agricultural losses (Basara *et al* 2019, National Centers for Environmental Information 2019) and the 2017 northern High Plains flash drought that significantly impacted wheat yields and increased the risk for wildfires (Gerken *et al* 2018, National Centers for Environmental Information 2019). Heatwaves have also been related to flash droughts, but this has been examined from a short-term anomaly perspective that is different than that employed in this study (Mo and Lettenmaier 2015). The Russia flash drought examined in this study is significant as it presents a flash drought precursor event that (1) yielded a rapidly desiccated land surface, (2) primed the

land-atmosphere interactions necessary for heatwave development and sensible heat advection, and (3) significantly contributed to a sequence of cascading and catastrophic impacts. Following the data and methods section, the results provide a quantitative analysis of land surface conditions associated with the initial rapid intensification toward drought, an assessment of the hydrometeorological response to the flash drought, and the spatial spread of desiccated land surface conditions across southwestern Russia.

2. Data and methods

Data from the Modern-Era Retrospective analysis for Research and Applications, Version 2 (MERRA-2; Gelaro *et al* 2017) were used to provide land surface variables for analysis of the flash drought and heatwave event across southwestern Russia with a spatial resolution of $0.5^\circ \times 0.625^\circ$. Daily values for each of the variables and derived quantities were averaged into pentads, then detrended and standardized using data from 1980–2016. The variables were detrended to evaluate anomalies in surface conditions after accounting for changes in the climate during the 37 years of the MERRA-2 dataset. In addition, variables were standardized to convert values to a statistical metric for domain-averaged calculations and for comparison of anomalies across the analysis window (May through September). The enhanced vegetation index (EVI; Huete *et al* 2002) from the Moderate Resolution Imaging Spectroradiometer (MODIS) onboard the NASA Aqua and Terra satellites was also used to leverage vegetative health as a proxy for the spatial propagation of land surface desiccation within the region of rapid drought development and heatwave onset during the summer months. The EVI was used as it reduces atmospheric influences on the canopy background signal (Huete *et al* 2002) and is more sensitive to drought than the normalized difference vegetation index (NDVI; Wagle *et al* 2014, Bajgain *et al* 2015). Further, EVI can accurately represent drought conditions via vegetative health as long as drought conditions persist for an extended period of time (e.g. greater than one month; Wagle *et al* 2014) and the drought events are severe (Bajgain *et al* 2015). EVI from Aqua was detrended and standardized with data from 2003–2019, while EVI from Terra was detrended and standardized with data from 2000–2019. The spatial resolution of the EVI used in the analysis was 0.05 degrees.

The spatial extent and temporal evolution of the flash drought event is analyzed using a comprehensive identification methodology in conjunction with the standardized evaporative stress ratio (SESR; Basara *et al* 2019, Christian *et al* 2019a, 2019b), which is a reanalysis-based variant of the satellite-derived evaporative stress index (ESI; Anderson *et al* 2007a, 2007b) that has also been used extensively in flash drought research (Otkin *et al* 2013, 2014, 2016, 2019, Nguyen

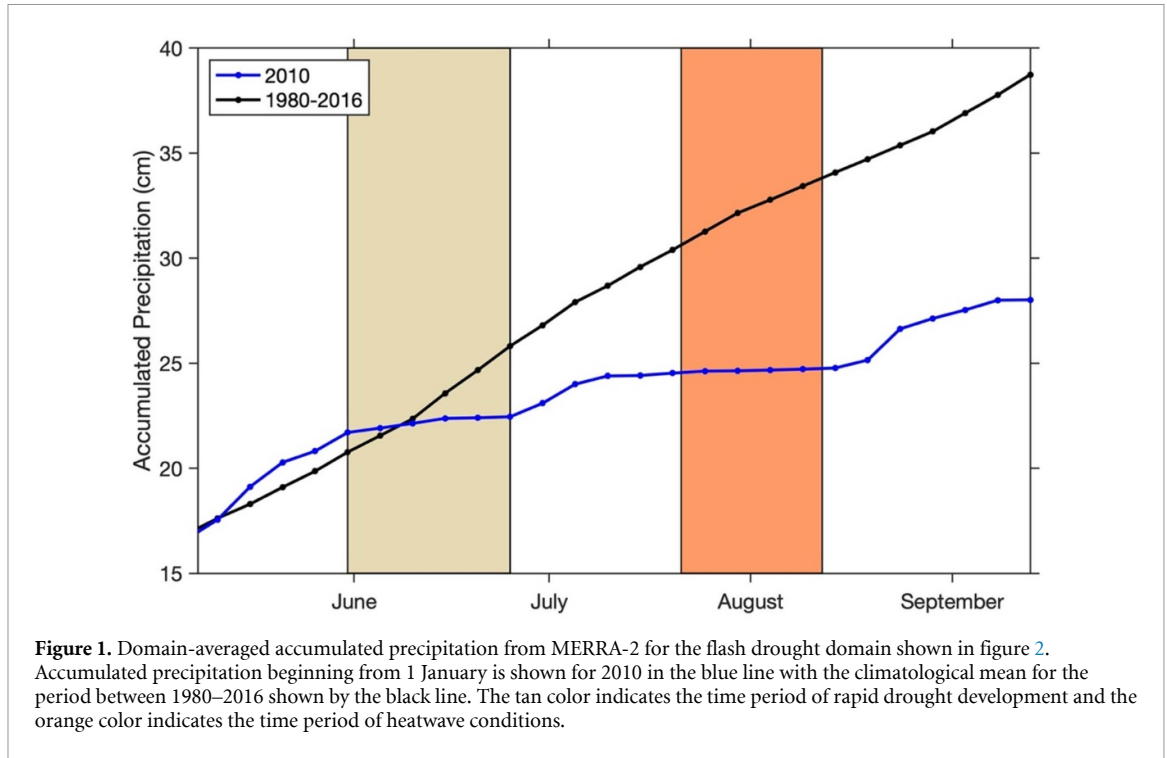


Figure 1. Domain-averaged accumulated precipitation from MERRA-2 for the flash drought domain shown in figure 2. Accumulated precipitation beginning from 1 January is shown for 2010 in the blue line with the climatological mean for the period between 1980–2016 shown by the black line. The tan color indicates the time period of rapid drought development and the orange color indicates the time period of heatwave conditions.

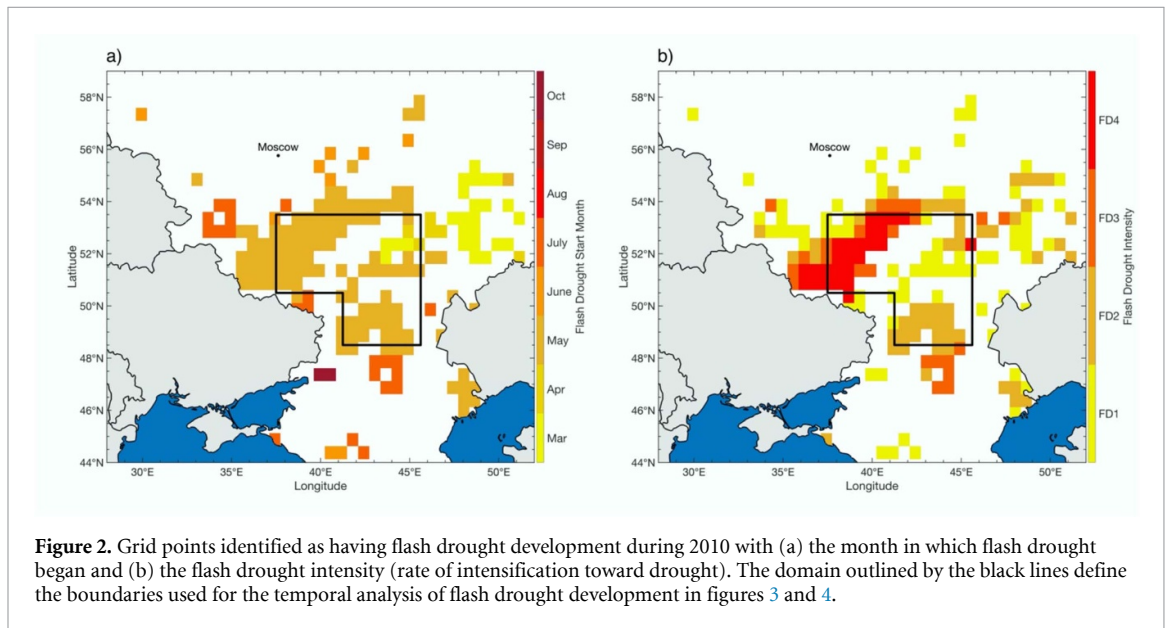


Figure 2. Grid points identified as having flash drought development during 2010 with (a) the month in which flash drought began and (b) the flash drought intensity (rate of intensification toward drought). The domain outlined by the black lines define the boundaries used for the temporal analysis of flash drought development in figures 3 and 4.

et al 2019). To calculate SESR, the ratio of ET and potential ET (PET; derived using the FAO Penman-Monteith equation; Allen et al 1998) from MERRA-2 were used to calculate daily values of the evaporative stress ratio (ESR). Mean pentad values of ESR were computed and standardized at each grid point:

$$SESR_{ijp} = \frac{ESR_{ijp} - \overline{ESR}_{ijp}}{\sigma_{ESR_{ijp}}}$$

where $SESR_{ijp}$ (referred to as SESR) is the z score of ESR at a specific grid point (i, j) for a specific pentad p , \overline{ESR} is the mean ESR at a specific grid point (i, j) for a specific pentad p for all years available in the gridded dataset, and σ_{ESR} is the standard deviation of ESR at

a specific grid point $SESR(i, j)$ for a specific pentad p for all years available in the gridded dataset. The temporal change in SESR was also calculated and standardized:

$$(\Delta SESR_{ijp})_z = \frac{\Delta SESR_{ijp} - \overline{\Delta SESR}_{ijp}}{\sigma_{\Delta SESR_{ijp}}}$$

where $(\Delta SESR_{ijp})_z$ (referred to as $\Delta SESR$) is the z score of the change in SESR at a specific grid point (i, j) for a specific pentad p , $\overline{\Delta SESR}$ is the mean change in SESR values at a specific grid point (i, j) for a specific pentad p for all years available in the gridded dataset, and $\sigma_{\Delta SESR}$ is the standard deviation of

SESR at a specific grid point (i, j) for a specific pentad p for all years available in the gridded dataset.

The flash drought identification criteria follow guidelines previously established for classification of rapid drought development with a dual emphasis on longevity and impact (Otkin *et al* 2018). Four criteria were used in total, with the first two focusing on the impacts of flash drought and the latter two emphasizing the rapid rate of intensification toward drought (Christian *et al* 2019a). The criteria are summarized as:

(1) A minimum length of five pentad changes in SESR, equivalent to a length of six pentads (30 d).

(2) A final SESR value below the 20th percentile of SESR values.

(3a) Δ SESR must be at or below the 40th percentile between individual pentads.

(3b) No more than one Δ SESR above the 40th percentile following a Δ SESR that meets criterion 3a.

(4) The mean change in SESR during the entire length of the flash drought must be less than the 30th percentile.

Percentiles for criteria 2 and 3 were taken from the distribution of SESR and Δ SESR at each grid point and specific pentad for all years in the dataset, while percentiles for criterion 4 were taken from the distribution of Δ SESR at each grid point for pentads that were encompassed within the flash drought event. The threshold percentile (30th percentile) in criterion (4) was slightly loosened compared to the threshold used for the climatological analysis of flash drought across the United States using a different dataset (25th percentile; Christian *et al* 2019a). The higher threshold (30th percentile) was used to better reveal locations that underwent flash drought development in this specific case study (especially for grid points with a mean overall change in SESR only slightly above the 25th percentile), while still requiring an overall rapid rate of intensification toward drought.

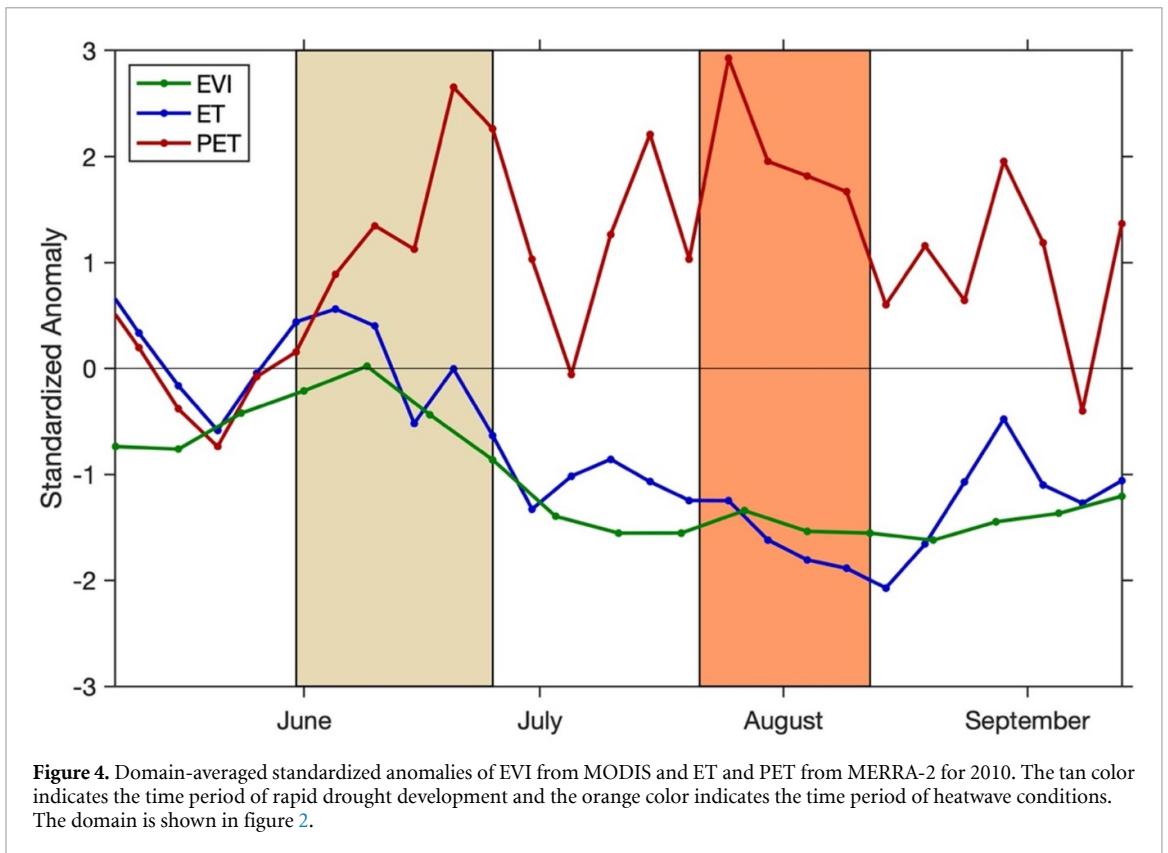
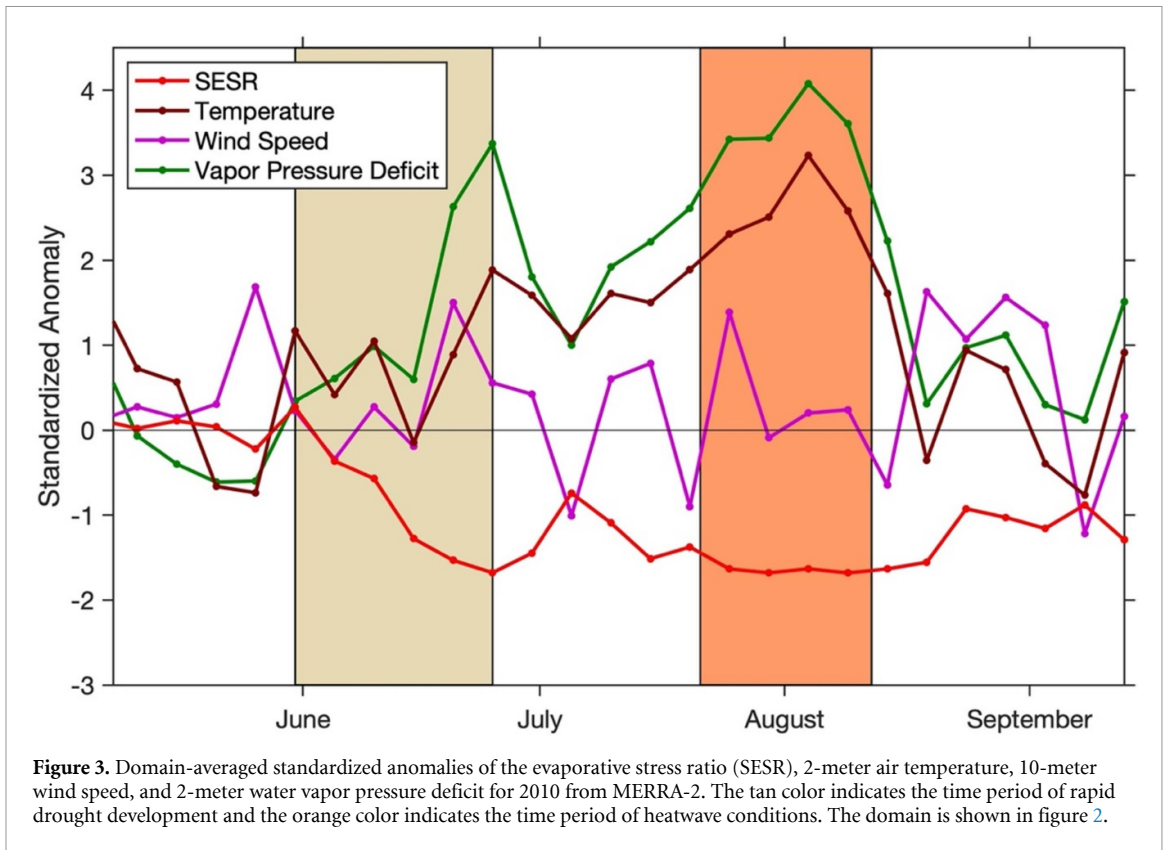
In addition to flash drought identification, the rate of intensification toward drought was classified into four categories using the mean SESR change (Δ SESR; criterion 4) using percentiles similar to those outlined in Christian *et al* (2019a): FD1—between the 25th and 30th percentile, FD2—between the 20th and 25th percentile, FD3—between the 15th and 20th percentile, and FD4—less than the 15th percentile.

3. Temporal evolution and spatial extent of flash drought

The primary flash drought development in southwestern Russia encompassed a region of approximately 260 000 km² (figure 2). Rapid drought development occurred concurrently across the area in the latter portions of May (figure 2(a)). This large-scale and simultaneous rapid drought intensification is in contrast to what was observed during the

2012 Great Plains flash drought in the United States whereby flash drought spatially propagated over several months (Basara *et al* 2019). However, the timing and location of the 2010 Russian flash drought was likely attributed to the presence of a quasi-stationary upper-level ridge and a different vegetation type across the region. The blocking high that began in June was expansive and covered a large area over much of eastern Europe and western Russia (Barriopedro *et al* 2011, Grumm 2011). This blocking feature set the foundational atmospheric conditions for rapid drought development with a lack of rainfall and enhanced evaporative demand (e.g. increased surface temperatures and reduced cloud coverage) at the land surface. However, the specific location of the flash drought event was likely due to ecosystems dominated by agriculture primarily south of 55°N (figure S1 (available at stacks.iop.org/ERL/15/094078/mmedia), Flach *et al* 2018). This is attributed to increased ET rates across the region and a more rapid depletion of root zone and near-surface soil moisture as compared to forested areas (figures S1, S2, and S3; Christian *et al* 2019a). This process rapidly lowers the evaporative fraction and limits the moderation of increased surface temperatures (figure S2). The higher surface temperatures further contribute to increased evaporative demand leading to a positive feedback and further desiccation of the terrestrial surface. As such, land-atmosphere coupling worked in tandem with the overlying synoptic environment to maximize rapid drought transition in this region. Areas north of 55°N in southwestern Russia are forest-dominated ecosystems and were shown to have normal and above-normal gross primary productivity during the summer of 2010 (figure S1, Flach *et al* 2018). Due to the deeper rooting depths of trees, forests can provide locally-sourced boundary layer moisture and moderate rapid drought development compared to an agriculturally dominated ecosystem. As a result, the region north of the primary flash drought area did not experience rapid drought development due to a slower decline of near-surface and root zone soil moisture over a couple of months (figure S3).

In addition to the very large spatial extent of the flash drought, the rate of intensification towards drought was unusually rapid even by the standards of flash drought. Previous research has classified the rate of drought intensification into four categories using the mean change in SESR at a given grid point during a flash drought: FD1—moderate flash drought, FD2—severe flash drought, FD3—extreme flash drought, and FD4—exceptional flash drought (Christian *et al* 2019a). While rapid drought development was classified as FD1 for much of the northeast portion of the domain, the southeastern section of the domain experienced flash drought categorized as FD2, and the western part of the study region saw the most rapid drought



development, reaching FD4 classification. The south-eastern portion of the domain was positioned within a temperature and precipitation gradient during the month of June (figures S4 and S5(b)), with higher

standardized temperature anomalies in the west and lower precipitation amounts in the east (south of 50.5°N). The alignment between these two gradients promoted the very rapid drought intensification

within this region, with the eastern part primarily driven by a deficit in precipitation and the western part supplemented by enhanced evaporative demand due to higher overall surface temperatures. For the western area of the study domain, below normal rainfall occurred in May prior to the onset of flash drought (figure S5(a)), with a further lack of rainfall during the rapid drought intensification period in June that was also coupled with above average surface temperatures (figure S4 and S5(b)). The coexisting deficit in precipitation and above-normal evaporative demand led to the rapid development of flash drought in this region.

The linkage between the flash drought event and heatwave event can be visualized by examining the temporal evolution of SESR and critical land surface variables that drive evaporative demand (figure 3). The domain used for analysis was selected to encompass a majority of the grid points that underwent flash drought during a similar period of time (figure 2(a)). The median start date of rapid drought intensification determined from identified flash drought grid points in the study domain was 31 May while the median end date of rapid intensification was 25 June. During this 25-day period, SESR began slightly above normal (indicating above normal environmental moisture conditions) and then rapidly declined to a value approaching 2 standard deviations below normal. In addition to the minimal rainfall during the month of June (figures 1 and S5(b)), surface temperatures and vapor pressure deficits were above normal, with near-normal wind-speeds. Each of these components contributed to high levels of evaporative demand on the land surface and led to rapid depletion of near-surface and root zone soil moisture (figure S2). Following the flash drought event, SESR slightly recovered during the early portions of July, but then slowly declined to values near two standard deviations below normal during the rest of the summer and the concurrent heatwave event. For the purpose of relating the temporal relationship between the flash drought and heatwave, heatwave conditions were defined where surface temperature exceeded 2 standard deviations above normal (figure 3).

Temperature values reached this threshold in late July and continued until early August. Extraordinarily high vapor pressure deficits were also experienced during this period, with values that were three standard deviations above normal during the heatwave event with peak values exceeding four standard deviations.

Rainfall and reduced evaporative demand that occurred in late June and early July contributed to the temporal delay between the end of rapid drought intensification and the onset of the heatwave (figure 1). While the mean accumulated precipitation across the study domain was minimal during this time period (approximately 2 cm), the rainfall was sufficient to effectively lower the anomalous

surface temperature and vapor pressure deficit for 3–4 pentads following the flash drought event (figure 3). As such, the excessive evaporative demand that occurred during the end of June (figure 4) temporarily moderated. It is important to note that the surface temperature was rapidly increasing to heatwave conditions at the end of the flash drought event. In a two pentad change in mid- to late June, standardized temperature anomalies increased approximately 2.0 standard deviations and standardized vapor pressure deficit anomalies increased an exceptional 2.8 standard deviations. Without the rainfall and associated moderation of evaporative stress on the environment, the focus of the heatwave event may have been shifted earlier into the summer and centered in the month of July. This could have exacerbated the environmental, economic, and societal impacts compared to the original heatwave event in late July and mid-August, given that the climatological surface temperatures across the region peak in mid-July (Grumm 2011). Nonetheless, the temporal evolution of the flash drought event and land surface variables reveal the rapid desiccation of the environment and the associated atmospheric response. With locally-sourced boundary layer moisture (i.e. ET) significantly diminished following the flash drought (figure 4), the land-surface was primed for land-atmosphere temperature coupling that enhanced the development of the heatwave event (Miralles *et al* 2014) in conjunction with the atmospheric conditions attributed to the quasi-stationary upper-level ridge (Barriopedro *et al* 2011, Grumm 2011).

4. The propagation of land surface desiccation during the flash drought and heatwave

The evolution and spread of land surface conditions across southwestern Russia during the flash drought and subsequent heatwave can be evaluated via changes in vegetative health conditions using the EVI. At the beginning of the rapid drought intensification period, evaporative demand increased approximately 1.2 standard deviations from near-normal to above-normal values (figure 4). During this same time period, a vegetative response was evident with increased ET and improved vegetation greenness to meet the evaporative demand of moisture at the land surface. However, as PET continued to rapidly increase into mid- and late June, plant available water was depleted due to a lack of rainfall (figures 1 and S2). A rapid decline of the vegetation conditions was evident during this period with an associated decrease in ET. The 1–2 pentad delayed response of vegetation to evaporative stress is similar to what has been observed in previous studies that have evaluated the lead time of evaporative stress with drought impact (Otkin *et al* 2013, Christian *et al* 2019a). The EVI reached its lowest values for the study domain

shortly after the rapid drought intensification period, and vegetation greenness remained well below normal throughout the remainder of the summer and into the heatwave event.

Spatial analysis of EVI reveals the connection between the initial flash drought region identified in this study and the broader area associated with the heatwave event (figure 5). Peak greenness was observed approximately 5–10 d into rapid drought intensification indicated by evaporative stress (figures 3, 4, and 5(a)). Areas to the north of the flash drought domain, including Moscow, also yielded EVI conditions that were well above normal during this time. However, in only 24 d after peak conditions were reached, EVI declined to well below normal across the study domain (figure 5(b)). The region surrounding Moscow and to the north of the study domain was also undergoing drought development, but at a slower rate than occurred within the initial flash drought region as seen by moderated EVI values. At the onset of the heatwave event, a respite in land surface degradation was visible in the flash drought region and locations north of 53.5°N (figure 5(c)) due to precipitation in early July (figure 1). However, the moderation in land surface conditions was temporary as the vegetation greenness decreased rapidly by the end of the heatwave throughout most of southwestern Russia (figure 5(d)).

An important part of this study is to reconcile the spatial differences between areas impacted by flash drought and the heatwave. The domain encompassing the region that concurrently underwent flash drought development covered an area of approximately 260 000 km². However, the region that had surface temperature anomalies in excess of 3 standard deviations extended farther north and west of the region characterized by rapid drought development (Twardosz and Kossowska-Cezak 2013). This mismatch between the biosphere response from flash drought and hydrometeorological extremes associated with the heatwave has been previously alluded to (Flach *et al* 2018). This north/east extension of the extreme surface temperatures associated with the heatwave is linked to the advection of air parcels within the synoptic anticyclonic circulation. In the period following rapid drought development and at the beginning of heatwave conditions, the wind direction was predominately southeasterly near Moscow (Galarneau Jr *et al* 2012, Witte *et al* 2011). Air parcels during this time followed trajectories directly over the flash drought region in which surface temperatures and vapor pressure deficits were exceptionally high (figure 3). In addition, dry soils associated with rapid drought development contribute to increased surface sensible heat fluxes. Strong torrents of sensible heat were advected from the flash drought region identified in this study to locations farther north (Schumacher *et al* 2019), aiding in enhanced evaporative demand and desiccation of the

land surface in these areas. This compounded onto the atmospheric conditions established by the upper-level ridge and the already struggling vegetation to prime the land surface for the extreme temperature anomalies associated with the heatwave event.

5. Summary and discussion

The 2010 event was characterized by a series of cascading hydrometeorological and environmental factors that produced catastrophic impacts across human and natural systems (figure 6). The atmospheric conditions imposed by the quasi-stationary upper level ridge (Barriopedro *et al* 2011, Grumm 2011; B11 and G11 in figure 6, respectively) inhibited rainfall (figure 1) and increased evaporative demand (figure 4) across the region for most of the summer. Flash drought development occurred across prime agricultural land in the Central, Volga, and Southern federal districts of southwestern Russia due to the coupled impacts of minimal precipitation and above-average PET (figure 2). The locality and critical phasing of the flash drought region embedded within the large-scale upper-level ridge was a result of increased ET and a rapid depletion of near-surface soil moisture as compared to a slower decrease of soil moisture in forested locations farther north (figures S1, S2, and S3). Near the terminus of the rapid drought intensification period, excessive stress on vegetation was evident across southwestern Russia and was most notable in the domain encompassing the flash drought region (figure 5(b)). The surface temperature was rapidly increasing to heatwave conditions (defined here as surface temperature greater than 2 standard deviations above normal) toward the end of the rapid drought development period at the end of June (figure 3), however, rainfall across the region moderated the evaporative demand for 2–3 weeks following the flash drought event (figure 1). After this short period of reprieve, little to no rainfall (<1 cm on average across the study domain) occurred between early July and mid-August (figure 1). This lack of rainfall, in combination with the previously desiccated land surface and poor vegetation health associated with the precursor flash drought event, permitted a rapid increase in surface temperature and vapor pressure deficit (figure 3). This was due to a rapid depletion of near-surface soil moisture via evaporation (and transpiration from the vegetation that was remaining and capable of photosynthesis) and resulted in a decrease of evaporative fraction by mid-July (figure S2).

As exceptionally high surface temperatures began to develop in late July, human mortality increased (Shaposhnikov *et al* 2014; S14 in figure 6). Further, an increased frequency of wildfires was observed (Bondur 2011, Witte *et al* 2011; B11 and W11 in figure 6, respectively), contributing to widespread loss of property and heightened levels of air pollution (Shaposhnikov *et al* 2014). By late July and early

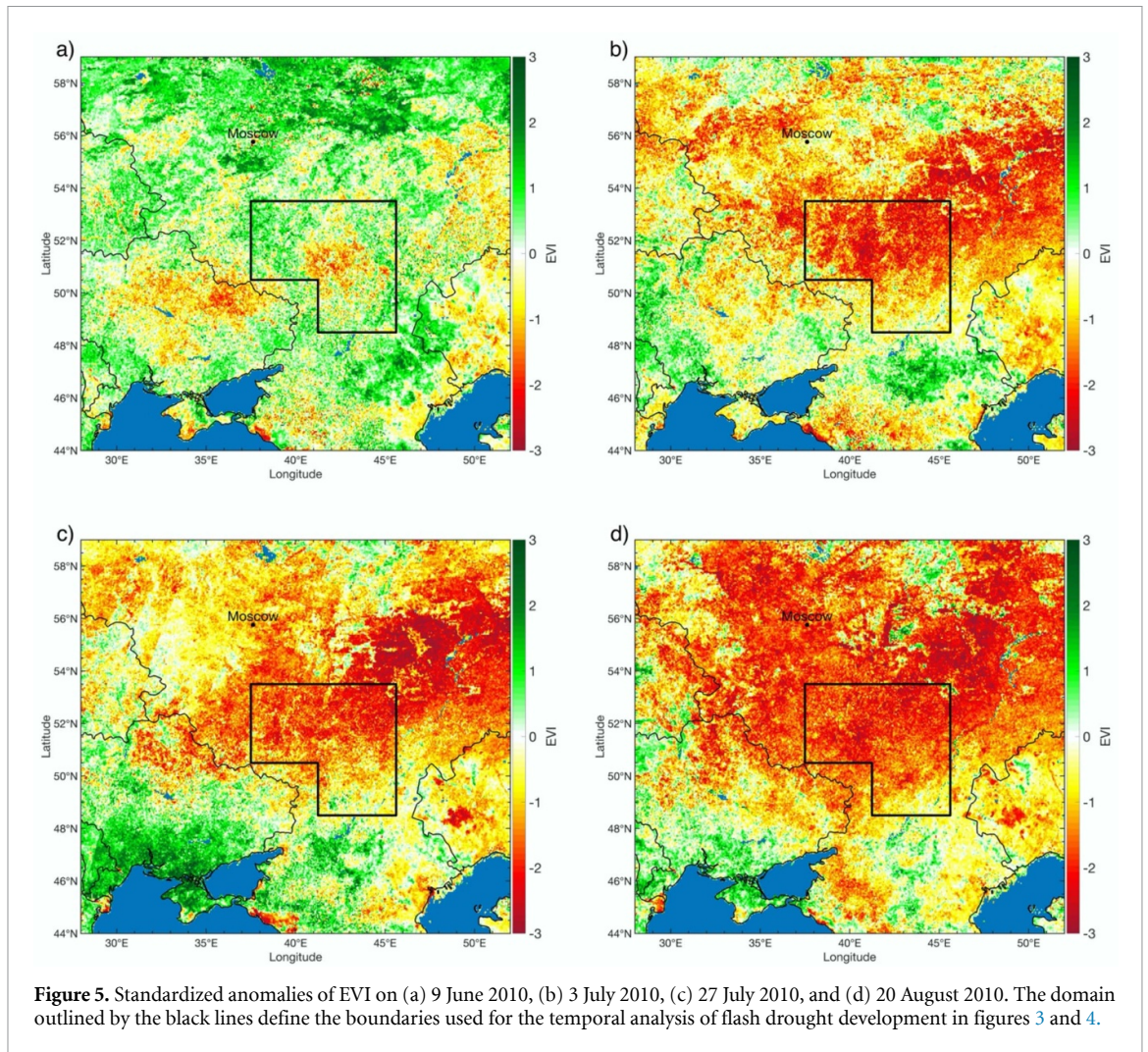


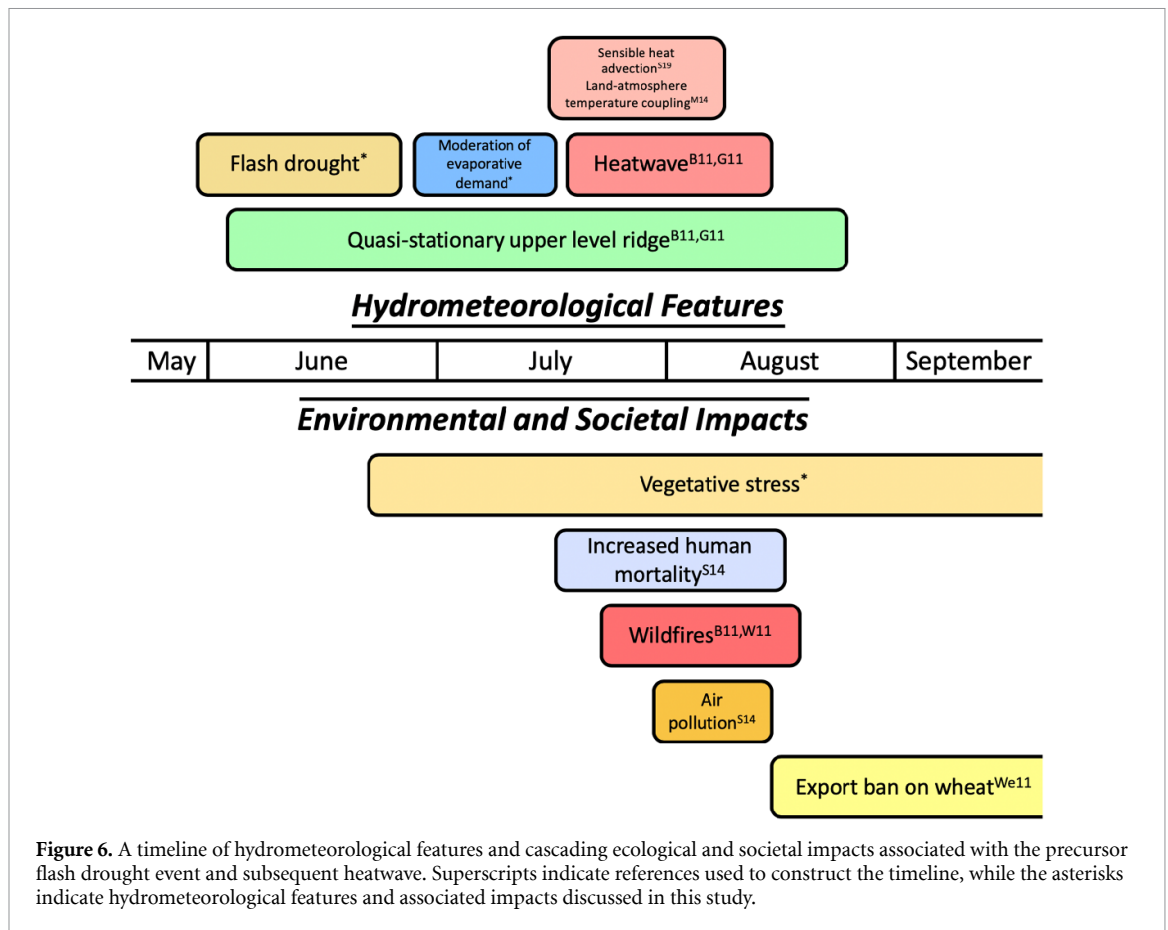
Figure 5. Standardized anomalies of EVI on (a) 9 June 2010, (b) 3 July 2010, (c) 27 July 2010, and (d) 20 August 2010. The domain outlined by the black lines define the boundaries used for the temporal analysis of flash drought development in figures 3 and 4.

August, land-atmosphere temperature coupling aided in the progressive development of heat in nocturnal residual layers (Miralles *et al* 2014; M14 in figure 6) and additional phasing between lower- and upper-level tropospheric circulations yielded sensible heat advection from the region that previously underwent flash drought toward locations farther to the north and west (Schumacher *et al* 2019; S19 in figure 6). Air-parcel trajectories around the lower-tropospheric high (Galarneau *et al* 2012, Witte *et al* 2011) and along areas of previously desiccated land surfaces supplemented the magnitude and spatially expanded the heatwave conditions across much of western Russia (Twardosz and Kossowska-Cezak 2013). By the time exceptionally high surface temperatures began to decline, agricultural regions were devastated (Wegren 2011), and an export ban was placed on wheat by the Russian government 15 August (Welton 2011; We11 in figure 6).

Traditionally, flash droughts have been associated with rapid soil moisture depletion, excessive stress on vegetation and ecosystems, and agricultural yield loss. This study provides additional insight into the linkage between flash drought and the rapid desiccation of the land surface with heatwave

development by (1) priming the land-atmosphere interactions necessary to supplement excessive surface temperatures while (2) simultaneously providing a focal point for the advection of sensible heat to promote heatwave development in other locations. As a result, flash drought events can serve as the connectivity between large-scale dynamic amplification and the terrestrial-atmosphere feedbacks associated with heatwaves (Miralles *et al* 2014, Schumacher *et al* 2019) and can initiate cascading social, ecological, and environmental impacts.

In the context of anthropogenic climate change, heatwaves similar to severity and extent of the Russian 2010 heatwave may occur with enhanced probability over the next twenty years across Europe (Russo *et al* 2015). Further, dry soils have also been shown to increase the risk for heatwaves in western Russia (Hauser *et al* 2016). Given that flash droughts are associated with a rapid depletion of soil moisture and can develop even when moisture conditions do not appear conducive for rapid drought development (Christian *et al* 2019b), flash droughts may be an important subseasonal phenomena to consider prior to the onset of heatwaves. This may become especially critical in a future climate



where spring soil moisture levels could become independent of maximum summer temperature anomalies in western Russia during summer blocking patterns (Rasmijn *et al* 2018). This would increase the likelihood for rapid drought development in the region when a combination of enhanced evaporative demand is coupled with minimal rainfall and persists for several weeks, especially in agricultural areas and climate transition zones that have an increased signal to land-atmosphere coupling (Koster *et al* 2004, Seneviratne *et al* 2006). As such, additional studies should investigate the role of flash drought and its associated land surface desiccation with heatwave development, especially in other locations across the globe that are susceptible to strong land-atmosphere coupling. Furthermore, future research should examine the climatological frequency of flash droughts that are precursors to heatwave events.

Acknowledgments

This work was supported, in part, by the NOAA Climate Program Office's Sectoral Applications Research Program (SARP) grant (NA130AR4310122), the Agriculture and Food Research Initiative Competitive Grant (2012-02355) from the USDA National Institute of Food and Agriculture, the USDA National Institute of Food and Agricultural (NIFA) Grant (2016- 68002-24967), the NASA

Water Resources Program grant (80NSSC19K1266), and the USDA Southern Great Plains Climate Hub. The data used from MERRA-2 in this study is available at <https://disc.gsfc.nasa.gov> and the data used from EVI is available at <https://search.earthdata.nasa.gov/search>. The flash drought data produced for this study is available upon request. The authors would also like to thank the anonymous reviewers for their feedback that improved the quality of this manuscript.

Data Availability Statement

The data that support the findings of this study are available upon reasonable request from the authors.

ORCID iDs

Jordan I Christian <https://orcid.org/0000-0003-2740-8201>

Jeffrey B Basara <https://orcid.org/0000-0002-2096-6844>

Eric D Hunt <https://orcid.org/0000-0001-7937-5611>

References

Allen R G, Pereira L S, Raes D and Smith M, 1998 Crop evapotranspiration - guidelines for computing crop water requirements - FAO Irrigation and drainage paper 56. FAO

- Anderson M C, Norman J M, Mecikalski J R, Otkin J A and Kustas W P 2007a A climatological study of evapotranspiration and moisture stress across the continental United States based on thermal remote sensing: 1. model formulation *J. Geophys. Res.* **112** 921
- Anderson M C, Norman J M, Mecikalski J R, Otkin J A and Kustas W P 2007b A climatological study of evapotranspiration and moisture stress across the continental United States based on thermal remote sensing: 2. surface moisture climatology *J. Geophys. Res.* **112** 1100
- Bajgain R, Xiao X, Wagle P, Basara J and Zhou Y 2015 Sensitivity analysis of vegetation indices to drought over two tallgrass prairie sites *ISPRS J. Photogramm. Remote Sens.* **108** 151–60
- Barriopedro D, Fischer E M, Luterbacher J, Trigo R M and García-Herrera R 2011 The hot summer of 2010: redrawing the temperature record map of Europe *Science* **332** 220–4
- Basara J B, Christian J I, Wakefield R A, Otkin J A, Hunt E H and Brown D P 2019 The evolution, propagation, and spread of flash drought in the Central United States during 2012 *Environ. Res. Lett.* **14** 084025
- Bondur V G 2011 Satellite monitoring of wildfires during the anomalous heat wave of 2010 in Russia *Izv. Atmos. Oceanic Phys.* **47** 1039–48
- Christian J I, Basara J B, Otkin J A and Hunt E D 2019b Regional characteristics of flash droughts across the United States *Environ. Res. Commun.* **1** 125004
- Christian J I, Basara J B, Otkin J A, Hunt E D, Wakefield R A, Flanagan P X and Xiao X 2019a A methodology for flash drought identification: application of flash drought frequency across the United States *J. Hydrometeorol.* **20** 833–46
- Flach M, Sippel S, Gans F, Bastos A, Brenning A, Reichstein M and Mahecha M D 2018 Contrasting biosphere responses to hydrometeorological extremes: revisiting the 2010 western Russian heatwave *Biogeosciences* **16** 6067–85
- Galarneau T J Jr, Hamill T M, Dole R M and Perlwitz J 2012 A multiscale analysis of the extreme weather events over Western Russia and Northern Pakistan during July 2010 *Mon. Weather Rev.* **140** 1639–1664
- Gelaro R *et al* 2017 The modern-era retrospective analysis for research and applications, version 2 (MERRA-2) *J. Clim.* **30** 5419–54
- Gerken T, Bromley G T, Ruddell B L, Williams S and Stoy P C 2018 Convective suppression before and during the United States Northern Great Plains flash drought of 2017 *Hydrol. Earth Syst. Sci.* **22** 4155–63
- Grumm R H 2011 The central European and Russian heat event of July–August 2010 *Bull. Am. Meteorol. Soc.* **92** 1285–96
- Hauser M, Orth R and Seneviratne S I 2016 Role of soil moisture versus recent climate change for the 2010 heat wave in western Russia *Geophys. Res. Lett.* **43** 2819–26
- Huete A, Didan K, Miura T, Rodriguez E P, Gao X and Ferreira L G 2002 Overview of the radiometric and biophysical performance of the MODIS vegetation indices *Remote Sens. Environ.* **83** 195–213
- Koster R D *et al* 2004 Regions of strong coupling between soil moisture and precipitation *Science* **305** 1138–40
- Miralles D G, Teuling A J, van Heerwaarden C C and de Arellano J V-G 2014 Mega-heatwave temperatures due to combined soil desiccation and atmospheric heat accumulation *Nat. Geosci.* **7** 345–9
- Mo K C and Lettenmaier D P 2015 Heat wave flash droughts in decline *Geophys. Res. Lett.* **42** 2823–9
- National Centers for Environmental Information 2019 Billion-dollar weather and climate disasters: overview NOAA NCEI (<https://ncdc.noaa.gov/billions/>)
- Nguyen H, Wheeler M C, Otkin J A, Cowan T, Frost A and Stone R 2019 Using the evaporative stress index to monitor flash drought in Australia *Environ. Res. Lett.* **14** 064016
- Otkin J A, Anderson M C, Hain C, Mladenova I E, Basara J B and Svoboda M 2013 Examining rapid onset drought development using the thermal infrared–based evaporative stress index *J. Hydrometeorol.* **14** 1057–74
- Otkin J A, Anderson M C, Hain C and Svoboda M 2014 Examining the relationship between drought development and rapid changes in the evaporative stress index *J. Hydrometeorol.* **15** 938–56
- Otkin J A, Anderson M C, Hain C, Svoboda M, Johnson D, Mueller R, Tadesse T, Wardlow B and Brown J 2016 Assessing the evolution of soil moisture and vegetation conditions during the 2012 United States flash drought *Agric. For. Meteorol.* **218–219** 230–42
- Otkin J A, Svoboda M, Hunt E D, Ford T W, Anderson M C, Hain C and Basara J B 2018 Flash droughts: a review and assessment of the challenges imposed by rapid-onset droughts in the United States *Bull. Am. Meteorol. Soc.* **99** 911–9
- Otkin J A, Zhong Y, Hunt E D, Basara J, Svoboda M, Anderson M C and Hain C 2019 Assessing the evolution of soil moisture and vegetation conditions during a flash drought–flash recovery sequence over the South-Central United States *J. Hydrometeorol.* **20** 549–62
- Rasmijn L M, van der Schrier G, Bintanja R, Barkmeijer J, Sterl A and Hazeleger W 2018 Future equivalent of 2010 Russian heatwave intensified by weakening soil moisture constraints *Nat. Clim. Change* **8** 381–5
- Russo S, Sillmann J and Fischer E M 2015 Top ten European heatwaves since 1950 and their occurrence in the coming decades *Environ. Res. Lett.* **10** 124003
- Schumacher D L, Keune J, van Heerwaarden C C, de Arellano J V-G, Teuling A J and Miralles D G 2019 Amplification of mega-heatwaves through heat torrents fueled by upwind drought *Nat. Geosci.* **12** 712–7
- Seneviratne S I, Lüthi D, Litschi M and Schär C 2006 Land–atmosphere coupling and climate change in Europe *Nature* **443** 205–9
- Shaposhnikov D *et al* 2014 Mortality related to air pollution with the moscow heat wave and wildfire of 2010 *Epidemiology* **25** 359–64
- Twardosz R and Kossowska-Cezak U 2013 Exceptionally hot summers in Central and Eastern Europe (1951–2010) *Theor. Appl. Climatol.* **112** 617–28
- Wagle P, Xiao X, Torn M S, Cook D R, Matamala R, Fischer M L, Jin C, Dong J and Biradar C 2014 Sensitivity of vegetation indices and gross primary production of tallgrass prairie to severe drought *Remote Sens. Environ.* **152** 1–14
- Wegren S K 2011 Food security and Russia's 2010 drought *Eurasian Geogr. Econ.* **52** 140–56
- Welton G 2011 The impact of Russia's 2010 grain export ban *Oxfam Research Report* pp 1–32 (<https://www.oxfam.org/en/research/impact-russias-2010-grain-export-ban>)
- Witte J C, Douglass A R, da Silva A, Torres O, Levy R and Duncan B N 2011 NASA A-train and terra observations of the 2010 Russian wildfires *Atmos. Chem. Phys.* **11** 9287–301